Effects of Temperature and Humidity on Atomic Force Microscopy Dimensional Measurement

TIAN WANG, CHENGFU MA, YUHANG CHEN,* JIARU CHU, AND WENHAO HUANG
Department of Precision Machinery and Precision Instrumentation, University of Science and Technology of China, Hefei, Anhui, 230026, China

KEY WORDS atomic force microscopy; dimensional measurement; humidity; temperature

ABSTRACT The influence of environmental factors on dimensional measurements of atomic force microscopy (AFM) was investigated experimentally. Measurements were taken with environmental control over a whole AFM chamber and a local sample chamber to highlight the influence of working conditions on the instrument itself. Both temperature and humidity were found to have a significant impact on pitch measurements of a two-dimensional grating. The effect of temperature on the behavior of the microscope itself is generally larger than the thermal expansion or contraction of the sample. The effect of humidity was further determined to be relevant to the scan direction and velocity. For precise AFM dimensional measurements, the possible influences of temperature and humidity must be carefully considered. *Microsc. Res. Tech. 78:562–568, 2015.*

INTRODUCTION

Surface nanometrology has emerged as an important field in nanoscience and nanotechnology. Among various tools for surface dimensional nanomeasurements, atomic force microscopy (AFM) is probably the most popular one owing to its prominent advantages, such as ultra-high spatial resolution, flexible working environment, simple sample preparation, and versatile operation modes (Yacoot and Koenders, 2008). However, many influencing factors, most of which have already been intensively investigated, should be considered to maximize the value of AFM in quantitative surface metrological applications. Such factors arise from various aspects of instrumentation components and operational methods. First, the probe tip has a finite size, which leads to complex geometrical coupling between the tip and the sample in surface data acquisition and causes considerable errors in determining the dimensional quantities of the sample (Chen and Huang, 2004; Gondran and Michelson, 2006). In addition, local tip–sample interaction forces may vary across the scan area because of different material properties at each sampling position. The inhomogeneous physical properties of the sample will then couple into the topography data (Piner and Ruoff, 2002; Yacoot et al., 2007). Remember that the interaction forces relevant quantities, such as cantilever deflection, oscillation amplitude, and frequency shift, are adopted for controlling the tip–sample distance. Second, AFM usually employs a piezo-scanner, which is affected by factors such as hysteresis, creep, and nonlinearity (Leang and Devasia, 2007). Closed-loop feedback control in three axes can be used to compensate for these error sources. However, for most conventional AFM measurements, such errors may still exist to a varying degree. Third, performance quality of all the microscope components can lead to considerable errors; for example, noise of the electric circuits and nonideal responses of the feedback controller (Anguiano et al., 1998). Last, the working environment, including factors like light, temperature, humidity, and electromagnetic field, can induce additional measurement errors (Lievonen et al., 2007).

The general environmental factors faced by an AFM instrument include temperature, humidity, pressure, and vibration. Of these, temperature and humidity are probably the most important. However, previous investigations on the influence of temperature mainly focus on the intrinsic thermal properties of the sample materials, such as the phase change of polymers (Jiang et al., 2003) and biological proteins (Schlierf and Rief, 2005). Moreover, thermal drift-induced distortions have been well studied (Henriksen and Stipp, 2002; Woodward and Schwartz, 1998). For the influence of humidity, much attention has been paid to its impact on capillary forces, friction, lubrication, etc. (Ando, 2000). These humidity-relevant forces subsequently cause complex nonlinear oscillations of the cantilever, which have also been intensively investigated (Sahagún et al., 2007; Zitzler et al., 2002). However, little concern has been paid to the effects of environment temperature and humidity on dimensional measurements. Intuitively, temperature can affect the AFM measurement from several aspects. First, temperature variations can cause thermal expansion or contraction

*Correspondence to: Yuhang Chen, Department of Precision Machinery and Precision Instrumentation, University of Science and Technology of China, Hefei, Anhui 230026, China E-mail: chenyh@ustc.edu.cn

Received 18 December 2014; accepted in revised form 1 April 2015
REVIEW EDITOR: Prof. Alberto Diaspro
Contract grant sponsor: "973" Project; Contract grant number: 2011CB932801; Contract grant sponsor: National Natural Science Foundation of China; Contract grant number: 51275503; Contract grant sponsor: Major National Scientific Instrument and Equipment Development Project; Contract grant number: 2011YQ040136.
DOI 10.1002/jemt.22509
Published online 20 April 2015 in Wiley Online Library (wileyonlinelibrary.com).

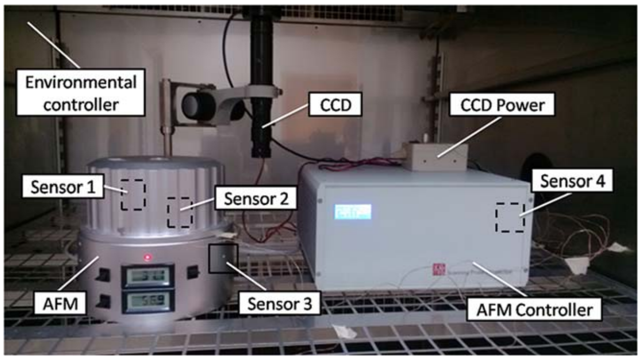

Fig. 1. Photograph of the experimental setup. Four temperature sensors were installed to monitor the temperature inside the environmental chamber. [Color figure can be viewed in the online issue, which is available at wileyonlinelibrary.com.]

of the sample. Second, thermal drift can induce image artifacts and thus affect the measurement of structural dimensions. Third, the behavior of the microscope components, such as piezoelectric properties of the piezo-scanner, may depend on the working temperature. As for humidity, capillary forces or lubrication effects, which are all relevant to humidity, cannot be ignored in scanning, and they will lead to different probe responses. Thus, humidity can also affect the quantitative geometric data obtained from the sample.

In this work, the influence of environmental factors on AFM dimensional measurements was studied experimentally, focusing on the contributions of temperature and humidity. Two types of practical conditions were considered. The first was environmental control of an overall AFM chamber containing the entire microscope. The second was the environmental control of a local chamber containing only the sample and the probe. In each series of experiments, we analyzed the effects of temperature and humidity on measuring the *X*- and *Y*-pitches of a two-dimensional (2D) calibration grating. These experimental investigations were carried out toward the purpose of highlighting and emphasizing the role of environmental factors on AFM dimensional characterization, especially when quantitative evaluation is necessary. However, the detailed influencing mechanism, which is relevant to almost all the instrumental components, was not concerned in these investigations.

EXPERIMENTAL METHODS

The first series of experiments were performed to imitate different ambient conditions that an AFM experiences in normal operations. Consequently, environmental control of a whole chamber containing the entire AFM instrument was applied, as shown in Figure 1. We used a commercial BY200 AFM (Benyuan Corporation). The environmental chamber (Tabai Espec Corporation) has nominal accuracy for temperature and humidity control of 0.1 °C and 0.1%, respectively. Four temperature sensors were installed inside the chamber, located beneath the AFM scanning head, at the side of the AFM head, at one side of the chamber, and at the chamber base. These sensors were monitored to ensure that the temperature around the microscope was homogenous and constant when acquiring the sample images.

Before data acquisition, temperature and humidity control procedures were programmed. Considering the common ambient operation environment, we programmed the control curves as schematically illustrated in Figure 2. The temperature was varied from 10 °C to 35 °C in an increment of 5 °C. Both increasing and decreasing temperature ramps were designed (see Fig. 2a). Such a temperature range was mainly chosen to represent the typical magnitudes in ambient air but not designed to study the temperature-relevant sample properties. For the relative humidity, the range was selected from 45% to 85%, with an adjustment step of 10%. Again, increasing and decreasing humidity ramps were designed (Fig. 2b). Note that the humidity range should be selected in a range that is not harmful to the AFM. Thus, for safe operation of a specified instrument, consulting the manufacturer's manual is recommended. To further examine potential synergistic influences of temperature and humidity, the increasing humidity ramp was repeated at two different temperatures, 25 °C and 30 °C. For each adjustment step, a waiting time of 2 h was set to allow the environment to stabilize, which can be confirmed by monitoring the installed sensors. After stabilization of the working environment at the assigned temperature and humidity, AFM imaging was executed. The probe here was a ContDLC cantilever (Budget Sensors), with the spring constant of 0.2 N m^{-1}, and the sample adopted in all the measurements was a 2D silicon calibration grating (NanoSensors). Among various dimensional quantities, the *X*- and *Y*-pitches of the 2D grating are supposed to be relatively insensitive to tip dilations. Consequently, we mainly analyzed the influences of temperature and humidity on the grating pitch measurement because the AFM-determined magnitude of this quantity should be relatively stable under tip wear. The scan size was 2 μm × 2 μm, with the sampling points set to be 256 pixels × 256 pixels.

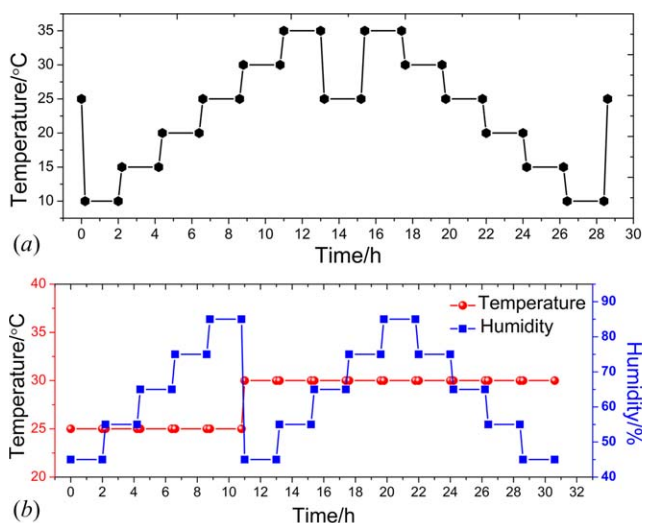

Fig. 2. Programmed temperature and humidity control curves in experiments. **a**: Temperature. **b**: Humidity. [Color figure can be viewed in the online issue, which is available at wileyonlinelibrary.com.]

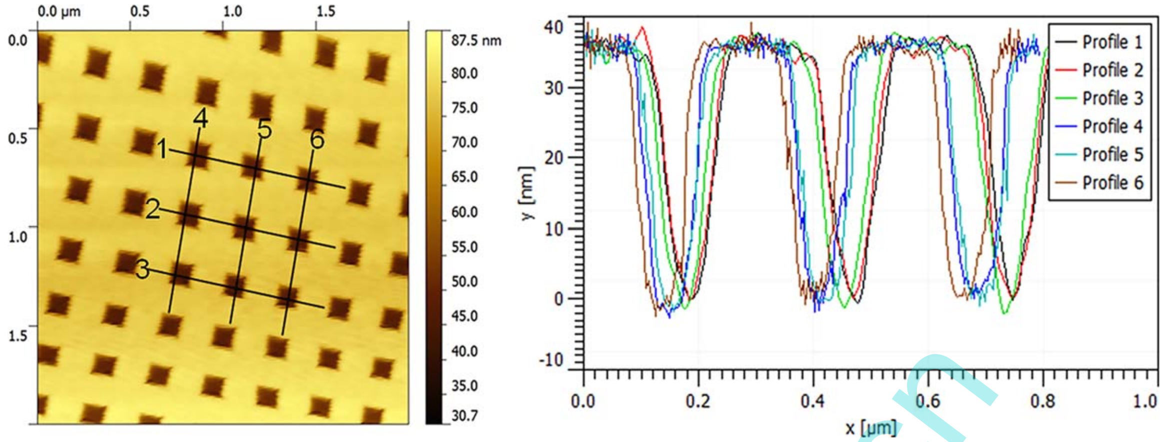

Fig. 3. Typical AFM images of the 2D calibration grating and pitch analysis from the section profiles. [Color figure can be viewed in the online issue, which is available at wileyonlinelibrary.com.]

With such settings, several grating periods were observable in the scanned area. The microscope was operated in contact mode, and the scan rate was 1.0 Hz.

The second series of experiments were performed with local environmental control over only a sample chamber. In this case, only the temperature and humidity around the probe and the sample were under control, whereas other AFM components were in ambient air. A commercially available AFM (SPA300HV, Seiko Instruments) equipped with a built-in sample holder environmental control module was used, and the probe was a silicon cantilever (SI-DF20, Seiko Instruments) with the spring constant of 16 N m^{-1}. Practical restrictions of the environmental controller embedded in the microscope allowed a temperature range from 25 °C to 55 °C, and a humidity range from 18% to 78%. The nominal temperature control accuracy is 1 °C. The programmed ramps were similar to the previous sets of experiments with the whole chamber environmental control. The ranges between the two different series of experiments are comparable, though they are not exactly the same.

RESULTS AND DISCUSSION

Figure 3 shows a typical AFM topographic image of the 2D grating. After analyzing subsequent images under the same environmental settings (Niu et al., 2010), drift-induced discrepancies were demonstrated to be insignificant in our experiments. To eliminate possible distortions induced by the scanner nonlinearity and cross-coupling between the *Z*-axis and *X–Y*-plane, we selected a central area containing 3 × 3 grating elements to measure the pitch at each environmental condition. The pitches in both *X*- and *Y*-directions were obtained by sectional profile analysis. From the extracted profiles as schematically sketched in Figure 3, the *X*- and *Y*-pitches can be calculated in form of their average means and standard deviations. We also applied Fourier transformation to determine the average grating pitches, and the results obtained by the two approaches were in close agreement. For clarity, we present here only the measured values from the sectional profile analysis.

Effect of Whole Chamber Environment

The influence of the whole chamber temperature on the measured grating pitch is shown in Figure 4. From the results, the temperature of the working chamber has an obvious influence on the dimensional measurement. Both the determined *X*- and *Y*-pitches change according to the temperature variation. Furthermore, the increasing and decreasing temperature ramps have similar trends, showing that the measured pitch decreases with higher environment temperature in general. In our case, the alterations of the measured pitches are approximately 1.2–1.5 nm °C^{-1} (*X*-direction) and 0.7–0.8 nm °C^{-1} (*Y*-direction). Note that an obvious minimum *Y*-pitch appears at 30 °C in the increasing temperature ramp. When acquiring images under that condition, we changed a new cantilever due to severe tip wear, and this may probably induce the local minimum in the measured *Y*-pitch.

As a rough estimation, the thermal expansion coefficient of silicon materials is approximately 2.6×10^{-6} °C^{-1}. Therefore, the dimensional difference considering purely the influence of thermal expansion or contraction is around 7.8×10^{-4} nm °C^{-1} for a grating pitch of 300 nm. The magnitude of the thermal expansion effect is, therefore, far smaller than that observed in our measurements. The experimental results indicate that the influence of temperature on the microscope itself, but not the thermal expansion or contraction of the sample, may be the dominant factor. In fact, the piezoelectric coefficient of the scanner has already been found to be closely relevant to the working temperature, and the coefficient may increase markedly with increasing temperature (Wang et al., 1998; Wolf and Trolier-McKinstry, 2004). To achieve the same elongation of the piezo-scanner, the drive voltage can be reduced when the temperature is higher. Without recalibration of scanner behavior, the apparent grating pitch will then be smaller at higher temperature. Such an effect should be taken

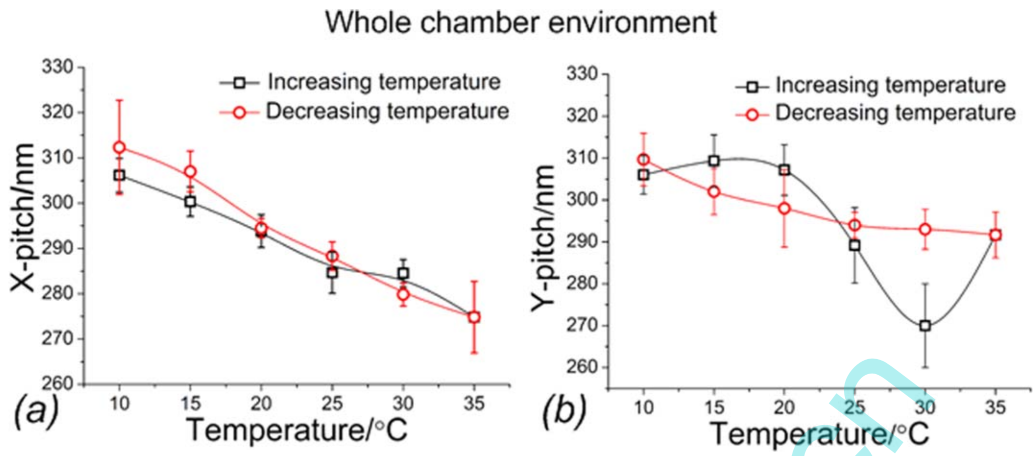

Fig. 4. Effects of the whole chamber temperature on the grating pitch measurement. **a**: *X*-direction. **b**: *Y*-direction. [Color figure can be viewed in the online issue, which is available at wileyonlinelibrary.com.]

into consideration, especially in cases where precise dimensional measurements are demanded.

Figure 5 shows how the chamber humidity typically affects the grating pitch measurement results. In this experiment, the temperature was 25 °C, and it was kept constant when altering the chamber humidity. Even though the standard deviation of the determined dimension is quite large, it can still be unambiguously concluded from the results that the measured grating pitches in the *X*-direction and the *Y*-direction decrease as the relative humidity increases. The large errors in the measured pitches are probably because of the imperfect geometry of the 2D grating. That is to say, the pitch measured at different cross-sections will intrinsically vary a lot. Here, the pitch reduction is approximately in the range of 0.9–1.2 nm (*X*-direction) and 4.1–8.0 nm (*Y*-direction) per 10% change of relative humidity. Such a magnitude demonstrates that relative humidity also does have obvious influence on the dimensional measurement. It is well known that humidity will affect the lubrication of tip–sample contact junction, which alters the frictional forces. In addition, capillary forces in ambient air are dependent on the humidity. Consequently, the interaction forces may be quite different as the humidity changes, which in turn cause different distortions of the determined dimensions. If the sample is immersed in liquid, then the influence of humidity is believed to be much weaker because of its ignorable effect on the tip–sample interactions. Another obvious indication from the experimental results is that the influence of humidity may be relevant to scan velocity. As can be seen in the figures, the overall trends and magnitude variations in the *Y*-direction are much more obvious than those in the *X*-direction. Note that the *X*-direction is set to be the fast scan direction in our experiments.

A further experiment was carried out to study the influence of coupling between temperature and humidity. By comparing the dependence of measured pitches on humidity, we can find that the two curves at 25 °C and 30 °C are well separated (see Fig. 6). Under the specified experimental conditions here, the influence of temperature seems to be larger than that of humidity. However, it is worth mentioning that the influence of humidity should be relevant to many other factors, such as operation modes and

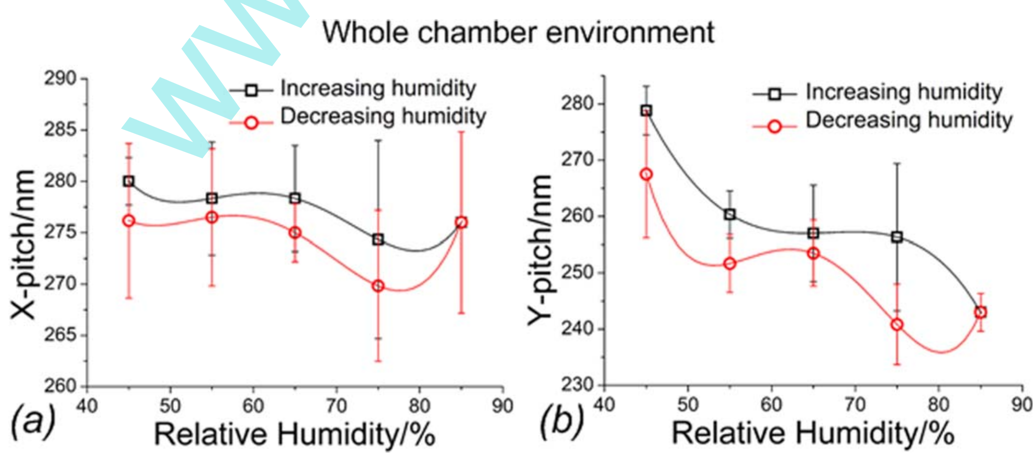

Fig. 5. Effects of the chamber humidity on the grating pitch measurement. **a**: *X*-direction. **b**: *Y*-direction. [Color figure can be viewed in the online issue, which is available at wileyonlinelibrary.com.]

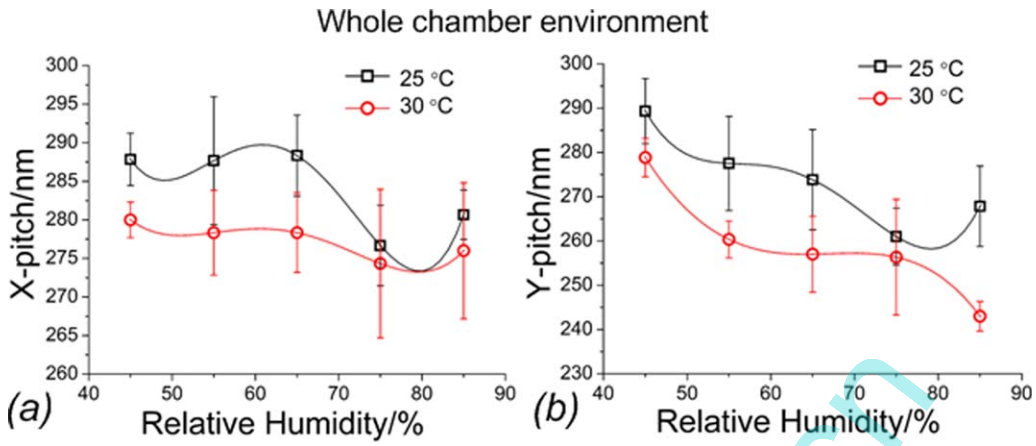

Fig. 6. Coupling effect of the whole chamber temperature and humidity on the grating pitch measurement. **a**: *X*-direction. **b**: *Y*-direction. [Color figure can be viewed in the online issue, which is available at wileyonlinelibrary.com.]

material properties of the samples. Depending on the surface hydrophilicity, the effect will be significantly different (Sirghi et al., 2006). Nevertheless, the possible influences of temperature and humidity should be paid careful attention in AFM-based dimensional metrology. When comparing the AFM results, it is, thus, necessary to provide enough information on the measurement environment.

Effect of Sample Holder Environment

We now investigate the effect of the local environment near the tip and sample only. As shown in Figure 7, the measured pitch in the *X*-direction increases, whereas the measured pitch in the *Y*-direction decreases as the assigned temperature of the sample chamber increases. Grating pitch variations in the two directions per unit temperature are determined to be 0.4–1.0 nm $^{\circ}C^{-1}$ and 0.7–0.8 nm $^{\circ}C^{-1}$ in the *X*- and *Y*-directions, respectively. Such magnitudes are again far larger than thermal expansion or contraction of the sample. However, it is difficult to determine specific reasons that these deviations should be different in the two directions. Further systematic investigation is necessary, but it is beyond the scope of this work. Here, we focused mainly on emphasizing possible environmental influence on AFM dimensional measurements.

Though the temperature ranges of the two different environmental controls are different, an overlapping range exists. Over the same temperature range, varying the whole chamber temperature (see Fig. 4) has a larger effect on the pitch measurement than varying the sample holder temperature (see Fig. 7). Results further demonstrate that the influence of temperature on the microscope itself is the dominant environmental factor in AFM dimensional measurements, and not the thermal expansion or contraction of the sample.

Figure 8 shows typical results of how the local humidity affects the grating pitch measurement. In fact, the trends are quite similar to those obtained with the whole chamber humidity control. The environmental humidity mainly affects the interactions of the tip–sample junction, whereas its influences on other AFM components seem to be negligible. So, both

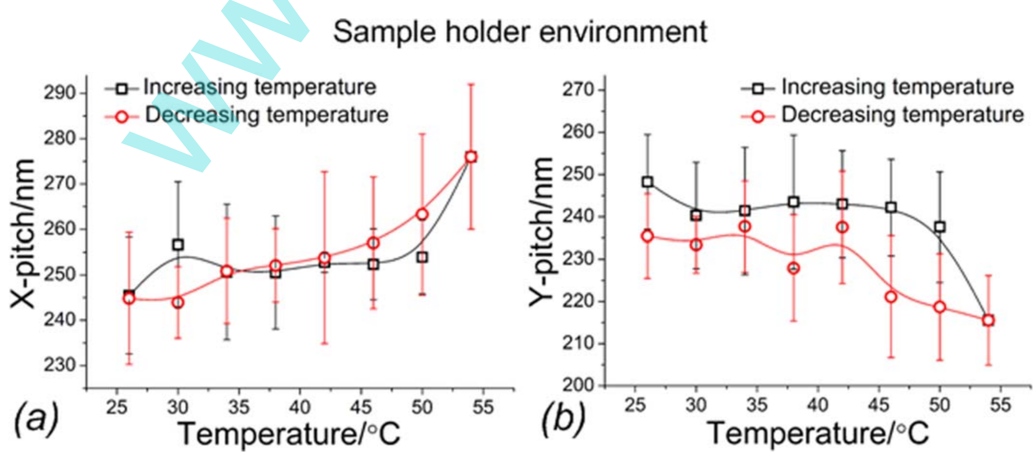

Fig. 7. Effects of the sample chamber temperature on the grating pitch measurement. **a**: *X*-direction. **b**: *Y*-direction. [Color figure can be viewed in the online issue, which is available at wileyonlinelibrary.com.]

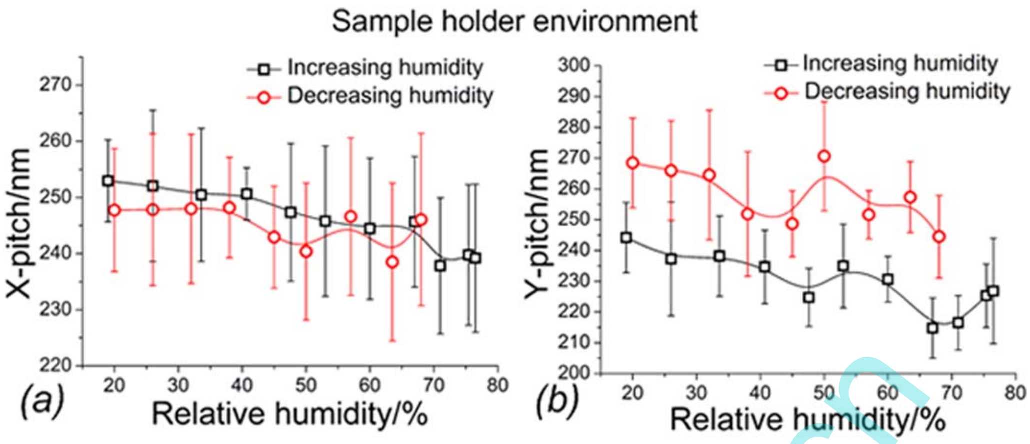

Fig. 8. Effects of the sample chamber humidity on the grating pitch measurement. **a**: *X*-direction. **b**: *Y*-direction. [Color figure can be viewed in the online issue, which is available at wileyonlinelibrary.com.]

whole chamber humidity control and local sample holder humidity control achieve nearly the same results. The measured grating pitches in the *X*- and *Y*-direction decrease as the relative humidity increases. Again, the variation trend and magnitude in the *Y*-direction are found to be much more obvious, which implies the influence of humidity depends closely on the scan velocity. Comparison of the humidity curves at 25 °C and 35 °C shows that they are well separated, as seen in Figure 9. Depending on the environmental temperature, the magnitude of the influence of humidity varies.

All above results demonstrate the obvious influence of environmental temperature and humidity on the dimensional measurements. However, such influence closely depends on the microscope itself, the sample under inspection, the mounted cantilever, and the operation mode. Thus, the magnitude of environmental effect is assumed to vary with different microscopes and experiments. If the accuracy of the dimensional measurement is of critical concern, then it is recommended to perform a detailed check of the possible distortions induced by environmental factors, as outlined in our experiments here.

SUMMARY AND CONCLUSIONS

Two types of experiments, those in which environmental control was held over the whole chamber and in which control was only held over the sample chamber, have been carried out to investigate the effects of temperature and humidity on AFM dimensional measurements. Using a silicon grating, both temperature and humidity are found to have obvious influences on the pitch measurements obtained via AFM. For example, in our experiments, the measured grating pitch changes approximately from 0.7 to 1.5 nm with every 1 °C temperature variation, and it changes from 0.9 to 1.2 nm (fast scan direction) and from 4.1 to 8.0 nm (slow scan direction) with every 10% variation of the relative humidity.

The effect of temperature on the behavior of the microscope itself is larger than the thermal expansion or contraction of the sample. In the case of environmental control of the whole chamber containing the

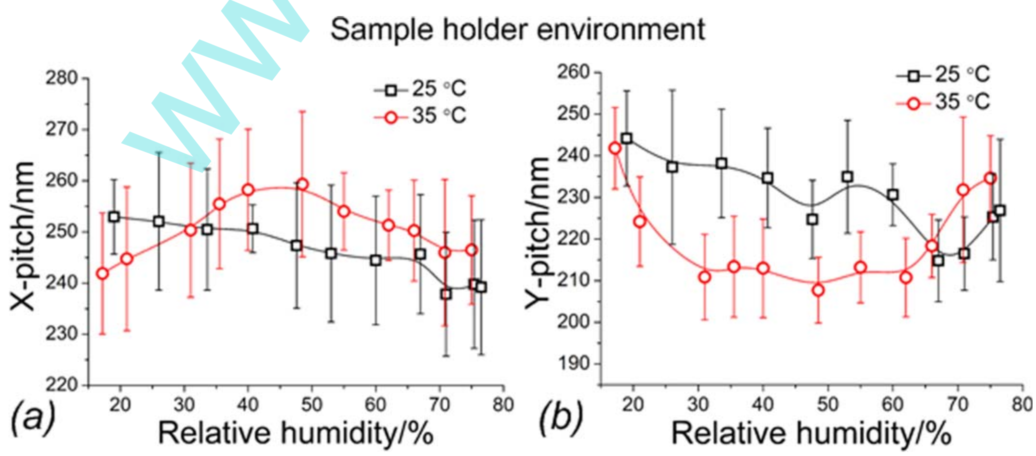

Fig. 9. Coupling effects of the sample chamber temperature and humidity on the grating pitch measurement. **a**: *X*-direction. **b**: *Y*-direction. [Color figure can be viewed in the online issue, which is available at wileyonlinelibrary.com.]

entire AFM system, the determined pitch decreases along with the increase of temperature, which is probably attributable to the alteration of the piezoscanner's piezoelectric coefficient. The effect of humidity on the grating pitch measurement is also quite obvious. Such effect is determined to be relevant to factors such as scan direction and scan velocity. Furthermore, it is believed to be relevant to material properties and AFM operation modes.

In precise AFM dimensional measurements, the possible influences of temperature and humidity should be taken carefully into consideration. Owing to the close dependence of these effects with the materials, operation modes, instrumental structures, and mechanical components, the requirement for further systematic investigations remains.

REFERENCES

Ando Y. 2000. The effect of relative humidity on friction and pull-off forces measured on submicron-size asperity arrays. Wear 238:12–19.

Anguiano E, Oliva AI, Aguilar M. 1998. Optimal conditions for imaging in scanning tunneling microscopy: Theory. Rev Sci Instrum 69: 3867–3874.

Chen Y, Huang W. 2004. Numerical simulation of the geometrical factors affecting surface roughness measurements by AFM. Meas Sci Technol 15:2005–2010.

Gondran CF, Michelson DK. 2006. Effect of probe tip size on atomic force microscopy roughness values for very smooth samples. J Vac Sci Technol A 24:1185–1190.

Henriksen K, Stipp SLS. 2002. Image distortion in scanning probe microscopy. Am Mineral 87:5–16.

Jiang Y, Yan DD, Gao X, Han CC, Jin XG, Li L, Chan CM. 2003. Lamellar branching of poly (bisphenol A-*co*-decane) spherulites at different temperatures studied by high-temperature AFM. Macromolecules 36:3652–3655.

Leang KK, Devasia S. 2007. Feedback-linearized inverse feedforward for creep, hysteresis, and vibration compensation in AFM piezoactuators. IEEE Trans Contr Syst Technol 15:927–935.

Lievonen J, Ranttila K, Ahlskog M. 2007. Environmental chamber for an atomic force microscope. Rev Sci Instrum 78:043703.

Niu D, Li J, Chen Y, Huang W. 2010. Comparative study on the nonperiodic and periodic gratings for scanning probe microscopy drift measurements. J Vac Sci Technol B 28:1070–1072.

Piner R, Ruoff RS. 2002. Cross talk between friction and height signals in atomic force microscopy. Rev Sci Instrum 73:3392–3394.

Sahagún E, García-Mochales P, Sacha GM, Sáenz JJ. 2007. Energy dissipation due to capillary interactions: Hydrophobicity maps in force microscopy. Phys Rev Lett 98:176106.

Schlierf M, Rief M. 2005. Temperature softening of a protein in single-molecule experiments. J Mol Biol 354:497–503.

Sirghi L, Szoszkiewicz R, Riedo E. 2006. Volume of a nanoscale water bridge. Langmuir 22:1093–1098.

Wang D, Fotinich Y, Carman GP. 1998. Influence of temperature on the electromechanical and fatigue behavior of piezoelectric ceramics. J Appl Phys 83:5342–5350.

Wolf RA, Trolier-McKinstry S. 2004. Temperature dependence of the piezoelectric response in lead zirconate titanate films. J Appl Phys 95:1397–1406.

Woodward JT, Schwartz DK. 1998. Removing drift from scanning probe microscope images of periodic samples. J Vac Sci Technol B 16:51–53.

Yacoot A, Koenders L. 2008. Topical review: Aspects of scanning force microscope probes and their effects on dimensional measurement. J Phys D Appl Phys 41:103001.

Yacoot A, Koenders L, Wolff H. 2007. An atomic force microscope for the study of the effects of tip—Sample interactions on dimensional metrology. Meas Sci Technol 18:350–359.

Zitzler L, Herminghaus S, Mugele F. 2002. Capillary forces in tapping mode atomic force microscopy. Phys Rev B 66:155436.